

Correlation of pre-operative cancer imaging techniques with post-operative macro and micro lung pathology images

G. Reines March^{1,2}, R. Sayer¹, S. Harrow³, C. Dick⁴, X. Ju¹, S. Marshall²

¹Medical Devices Unit, West Glasgow Ambulatory Care Hospital, NHS Greater Glasgow and Clyde, Glasgow G3 8SJ (UK)
²Hyperspectral Imaging Centre, Dept. of Electronic and Electrical Engineering, University of Strathclyde, Glasgow G1 1XW (UK)
³Clinical Oncology, The Beatson West of Scotland Cancer Centre, NHS Greater Glasgow and Clyde, Glasgow G12 0YN (UK)
⁴Clinical Pathology, Queen Elizabeth University Hospital, NHS Greater Glasgow and Clyde, Glasgow G51 4TF (UK)

Background

The overall goal of this project is to ascertain whether **a given PET radiotracer reliably and accurately identifies an active cancerous region** within the gross tumour volume. The only means to assess it is to compare the PET signal with the gold standard of histopathology. To allow for this comparison both images need to be **spatially aligned** or registered.

However, lung tissue undergoes several **deformations** following surgical resection and pathological processing. Therefore, these distortions need to be taken into account in order to obtain a truthful mapping. Moreover, PET signals are intrinsically 3D, whereas histopathology slices are planar images. In order to overcome this problem, **2D slices have to be stacked together** to reconstruct the original volume prior to registration.

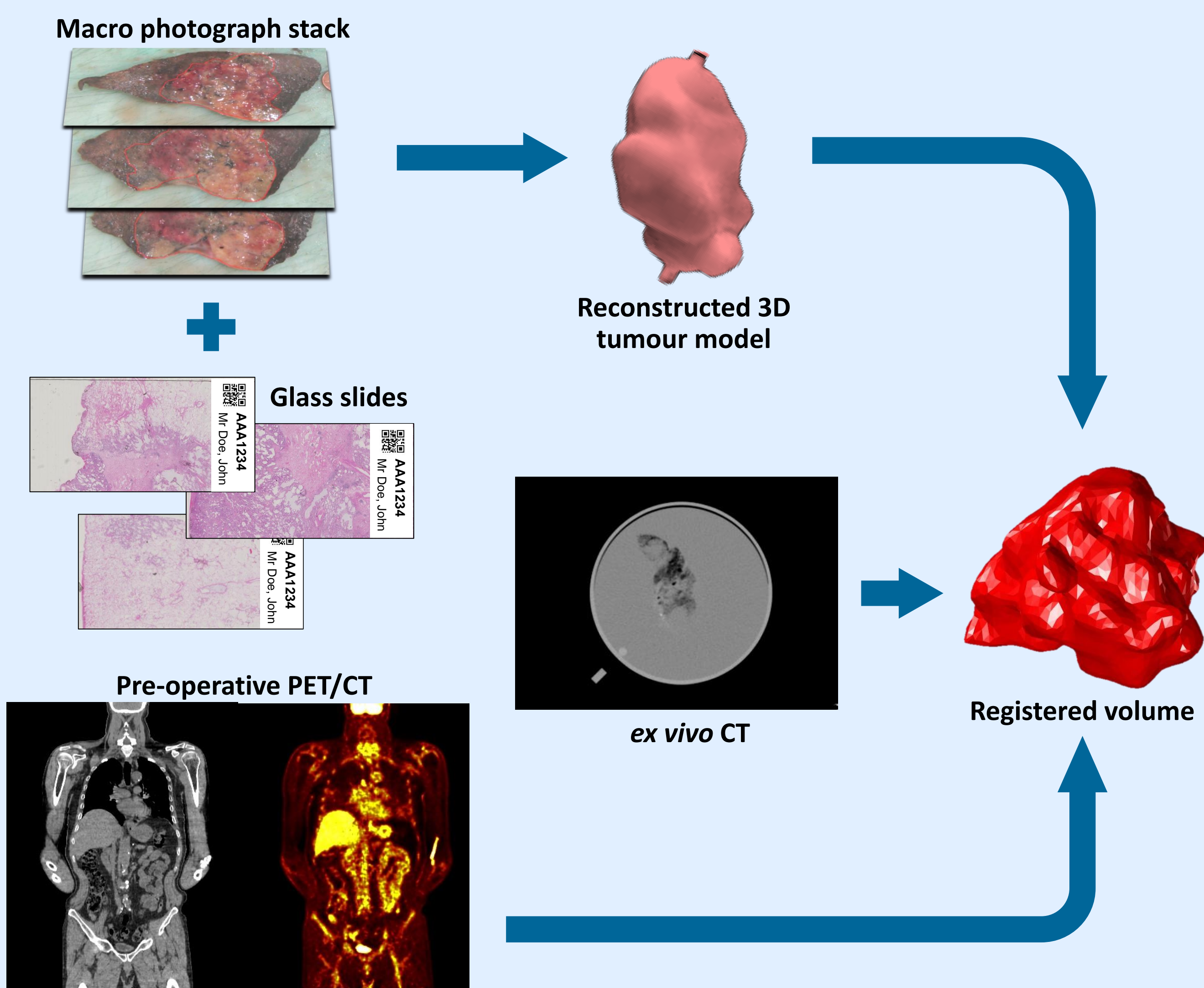


Figure 1: diagram showing all the steps in the image acquisition and processing workflow

Materials and Methods

Phantom study

A synthetic phantom has been used to test the different volume reconstruction algorithms, made from an aqueous mixture of **agar powder** and **aluminium oxide**.

Characteristics:

- Its design recreates an **anatomical** model
- Includes different **morphologic features**, to test and challenge the algorithms used
- Texture similar to **lung tissue**

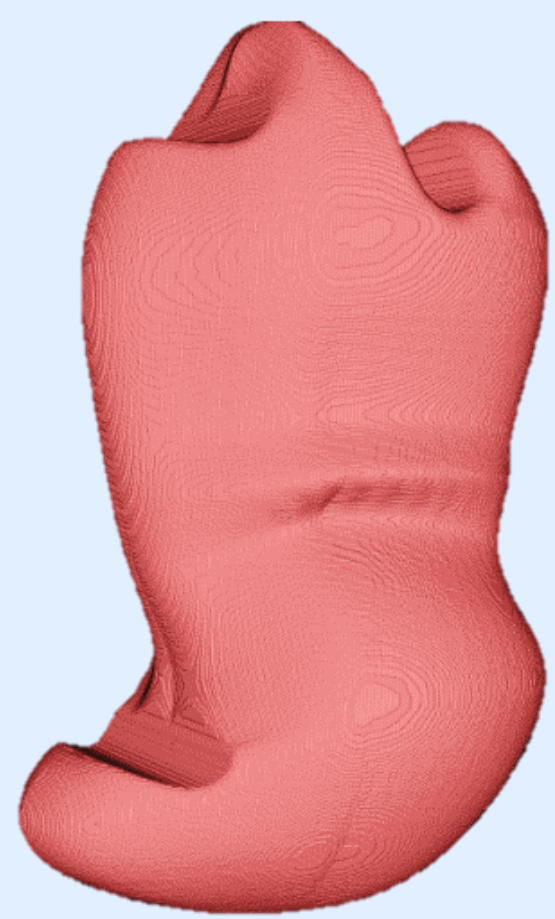


Figure 2: CAD model of the phantom

A custom-made, re-usable mould was produced with 3D printing technology to cast the model. The presence of aluminium oxide makes the phantom visible in the **x-ray** and **visible** regions of the spectrum.

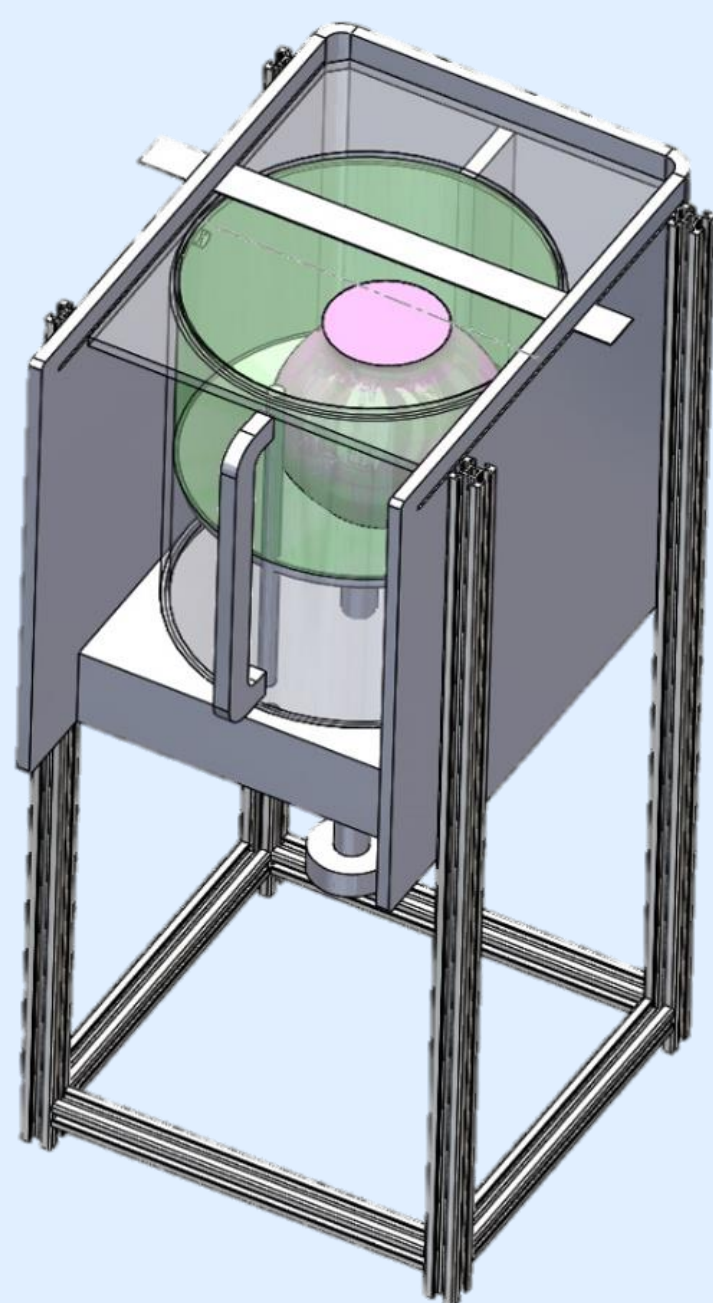


Figure 3: CAD model of the slicing rig

Slicing rig

Pathological dissection is usually performed **free-hand** by a pathologist. Although faster, this method is less precise in terms of slice thickness uniformity, and the lung tissue is more likely to tear and deform.

For this reason, a bespoke **soft tissue slicing rig** has been designed. The tissue to be sliced, which is **fixed in agarose**, is pushed upwards using a precise threaded plunger. A pathology knife is then used to perform a **clean, flat cut**. At this point, the slice is **photographed** and stored away for further processing. This procedure is repeated until the whole tissue of interest has been imaged.

Results

Micro- and macroscopic registration

The initial approach used to fuse the microscopy slides with the gross specimen photographs was based on **manual landmark** detection. Common features which could be identified on both datasets (e.g. vessels, airways, contours) were selected and matched. Then, using a **non-rigid registration algorithm** (moving least squares), and imposing the selected landmarks as hard constraints, the microscopy image was deformed to match the macro photograph.

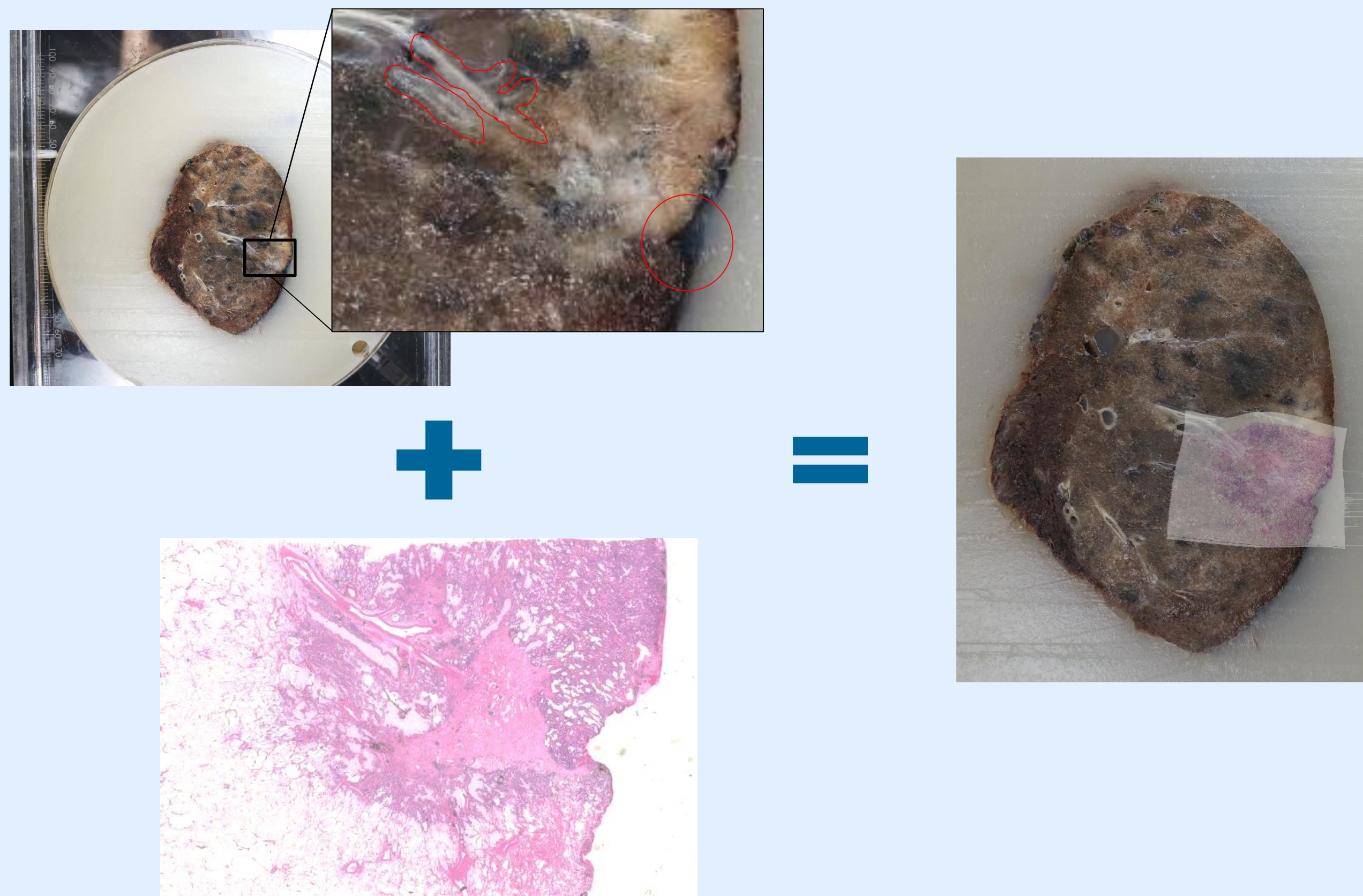


Figure 4: micro and macro image registration workflow

Tumour volume reconstruction from gross pathology data

Although digital pathology images can easily achieve sub-millimetre pixel sizes, the axial sampling frequency is severely limited by how thin we can dissect our specimen, which for lung tissue it is about 5 millimetres. Therefore, a powerful **interpolation algorithm** is required to reconstruct a continuous 3D shape from this anisotropic dataset. Several **interpolation kernels** have been tested with a bespoke tumour phantom, to assess which one performs better and returns the most truthful reconstruction in terms of shape and volume recovery.

From all kernels evaluated, **nearest neighbour** interpolation returns the most accurate overall volume, whereas **second-order bi-cubic spline** achieves the highest degree of similarity in terms of shape reconstruction.

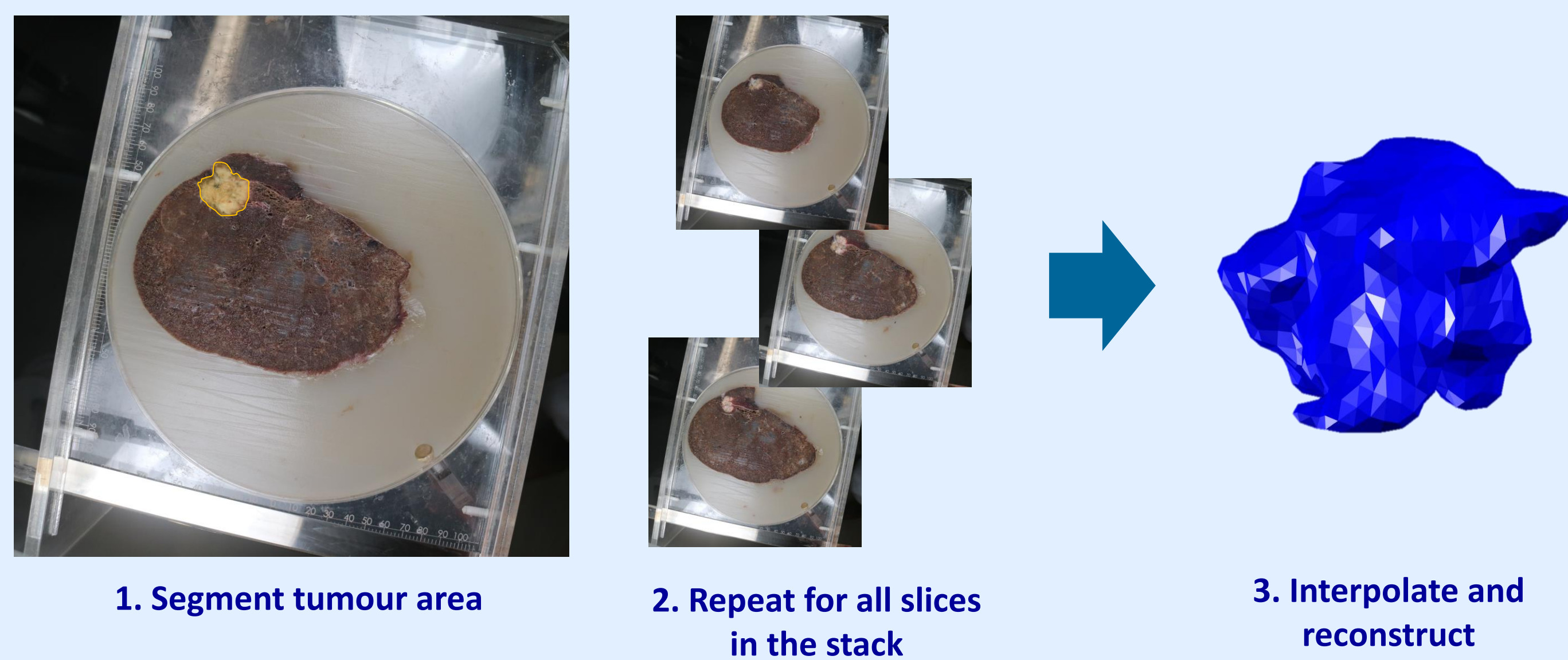


Figure 5: tumour 3D reconstruction workflow

Several **semi-automatic segmentation routines** have been explored to speed up the delineation process, which is a highly time-consuming step. Taking manual segmentation from an experienced pathologist (CD) as ground truth, we have explored **colour thresholding**, **active contours** and **region growing** segmentation algorithms, the latter giving the most accurate results to date.

Future work

Next planned steps include the **registration** of free-breathing pre-operative CT tumour volume to the reconstructed 3D pathology model. This will be used as a preliminary result and proof of concept. Upon successful development and testing of a **non-rigid volume-to-volume registration algorithm**, we will then fuse the pathology volume to respiratory-gated (4D) PET/CT scans. This will ultimately allow us to **match microscopic pathological features to its pre-operative functional map**.

Acknowledgements: